Transactions of the Indian National Academy of Engineering (2023) 8:221–233
https://doi.org/10.1007/s41403-023-00389-9

ORIGINAL ARTICLE

Numerical Study on NO_x Emissions from Jet A–Air Detonations

M. S. Karthikeyan Iyer[1] · Ashlesh Dahake[1] · Ranjay K. Singh[1] · Ajay V. Singh[1]

Received: 18 June 2022 / Accepted: 26 January 2023 / Published online: 6 February 2023
© Indian National Academy of Engineering 2023

Abstract
The propulsive application of detonation-based engines has been well recognized since detonations offer an environment for efficient burning of a given fuel–oxidizer mixture with increased efficiency. The use of liquid hydrocarbon fuels is necessary for these advanced detonation-based combustors to resolve problems associated with the fuel payload and operating cost. However, using jet fuels for such combustors is a challenging task since the propagation limits and stability of detonation waves in such scenarios are not known and warrant further investigation. In addition, NO_x emissions from such systems have so far received less attention. Since the emissions control protocol has become more stringent for air-breathing engines, it is necessary to understand the NO_x chemistry of real distillate fuels in a detonating environment. For the mixtures and operating conditions featuring promising detonability, NO_x formation in the detonation wave has been simulated using a detailed HyChem Jet A reaction model combined with the NO_x model of Glarborg et al. The purpose of the present study is to quantify the effect of initial temperature and initial pressure on NO_x emissions for Jet A–air detonations over a wide range of initial conditions. The effect of dilution on NO_x emissions was also investigated in the presence of inert diluents such as argon and helium. The observation from the computed results indicates that the addition of inert diluents significantly reduces the NO_x emissions, with the comparative difference in NO_x suppressing ability between argon and helium being insignificant. The present study lays the groundwork for the optimized operation of liquid hydrocarbon-fuelled detonation-based engines and enables an insight into the potential measures that can be employed for reduced NO_x emissions in such devices.

Keywords Jet A · NO_x · Detonations · Detonation-based engines

List of Symbols

Δ_i	Induction zone length (mm)
τ_i	Induction delay time (μs)
Δ_r	Reaction zone length (mm)
τ_r	Reaction time (μs)
Δ_{recom}	Recombination zone length (mm)
τ_{recom}	Recombination time (μs)
T_{CJ}	Post-detonation temperature (K)
T_{VN}	Post-shock temperature (K)
P_{CJ}	Post-detonation pressure (atm)
P_{VN}	Post-shock pressure (atm)
M_{CJ}	CJ detonation Mach number
X_i	Mole fraction of *i*th species
σ	Thermicity (1/μs)
NO_x	Oxides of nitrogen ($NO + NO_2 + N_2O$)
T_0	Initial temperature (K)
P_0	Initial pressure (atm)
φ	Equivalence ratio (−)

✉ Ajay V. Singh
ajayvs@iitk.ac.in

[1] Department of Aerospace Engineering, Indian Institute of Technology Kanpur, Kanpur 208016, India

Introduction

Detonation-based engines have gained increased popularity in recent years as they offer more advantages when compared to conventional gas turbine engines. Detonation-based engines have higher thermodynamic efficiency (theoretically twice as much as the Brayton cycle) when compared to conventional gas turbine engines and are more robust and simpler (Heiser and Pratt 2002). These engines operate under a pressure gain combustion process and remove the necessity for compressing a given fuel–oxidizer mixture. This helps in improving the power-to-weight ratio of the engine and also results in a moderate cost of operation due to increased efficiency. The operation of detonation-based combustors has been extensively investigated for gaseous fuels, and very few works report their operation with liquid hydrocarbon fuels (Kailasnath 2006; Dahake and Singh 2022a, d; Iyer

et al. 2022; Iyer and Singh 2022a). To keep operating costs low and address the issues associated with usage, transportation, and storage, it is imperative to use real distillate fuels like Jet A for detonation-based combustors. Real distillate fuel like Jet A also acts as an excellent endothermic liquid hydrocarbon fuel and can act as an active cooling system to reduce the severe heat loads due to aerodynamic heating. Detonation-based combustors for civil aviation are expected to use real distillate fuels like Jet A for propulsion applications. However, one of the difficulties faced by Jet A, which is also true for other real distillate fuels, is that its ignition kinetics may be too slow for its application in detonation-based combustors. Another challenge with detonation-based combustors is that the associated temperatures could be very high, ~ 2800 K to 3200 K, which could lead to structural failure in the absence of complex cooling mechanisms and could lead to higher NO_x emissions. To address the issues related to slower ignition chemistry and cooling of these engine cores, various researchers have suggested sensitizing the fuel–oxidizer mixture with ignition promoters (Magzumov et al. 1998; Chen et al. 2011; Kumar et al. 2021; Crane et al. 2019). Kumar et al. (2021) have shown that the combustor temperature can be controlled within desired operating limits by doping the fuel–oxidizer mixture with ignition promoters in the presence of inert diluents. Most of the previous studies on gaseous detonations have shown the essence of the detailed chemical kinetic model in the accurate predictions of critical parameters involved in the detonation process (Westbrook and Urtiew 1982; Westbrook 1982). Although a lot of research is being actively conducted worldwide on detonation-based combustors, NO_x emissions from such systems have so far received very little attention and warrant further investigation (Anand and Gutmark 2019). Hence, it is essential to investigate the NO_x emissions from detonation-based combustors over a wide range of operating conditions.

The NO_x emission protocol has become more stringent in the past few years for the aviation industry. Nitrogen oxides, collectively termed NO_x, are essentially formed in all combustion and high-temperature industrial processes and are designated as harmful pollutants since they are responsible for acid rains (NO and NO_2) and participate in the generation of photochemical smog (NO and NO_2). On the other hand, N_2O has a significant impact on the ozone layer and is a greenhouse gas. In almost all practical engines, Nitric oxide (NO) is the most dominant species in NO_x, and its concentration is substantially higher than nitrogen dioxide (NO_2) and nitrous oxide (N_2O). Primary methods for NO_x abatement include burning a given fuel–oxidizer mixture in lean conditions and using the method of exhaust gas recirculation. Several other approaches that can be employed for NO_x reduction include staged combustion, spark time-shifting, and altering the design of the combustor and fuel nozzle. However, these methods may or may not be feasible for a detonation-based combustor because of the complexity associated with such systems. Several mechanisms or reaction pathways could lead to the formation of oxides of nitrogen in a combustion system. Earlier works suggest that in the absence of fuel NO_x, the formation of NO arises from the fixation of N_2 in the combustion air (Glarborg et al. 2018). Dominant reaction pathways for NO production include the thermal NO and the prompt NO mechanism. In addition, NO formation could also occur through N_2O, $O + N_2 (+M) \rightarrow N_2O (+M)$, or NNH, $H + N_2 (+M) \rightarrow NNH (+M)$ routes (Glarborg et al. 2018).

Djordjevic et al. (2018) have conducted a numerical study to investigate the methods of NO_x control in pulse detonation engines (PDEs). They observed that for a given fuel–oxidizer mixture, steam dilution or nitrogen dilution is a better method to control NO_x emissions than using lean mixtures. They also pointed out the applicability of this technique only to a limited extent as the detonability of a given mixture was found to be severely affected. Xisto et al. (2019) measured the CO_2 and NO_x emissions from an intercooled PDC (pulsed detonation combustor) turbofan engine, where they suggested controlling NO_x emissions using stratified charges. Hanraths et al. (2018) also performed a numerical study for predicting NO_x emissions from a PDE. In a more recent study, Dahake and Singh (2021) studied NO_x emissions from a synthetic biofuel for applications in detonation-based engines. In a subsequent study, they also studied the effect of fuel sensitization on the NO_x emissions from a biofuel under detonating conditions (Dahake and Singh 2022b, c). Saggese et al. (2020) investigated the NO_x formation from stretch stabilized premixed laminar flames of methane and Jet A. For modeling the real fuel combustion chemistry of Jet A and to predict NO_x emissions in quasi-one-dimensional laminar flames, the HyChem model was combined with the Glarborg NO_x model by the authors, and the model was validated with the experimental data (Saggese et al. 2020). For all conditions tested numerically, they obtained reasonably good agreement with the experimental results, especially for fuel-lean and stoichiometric conditions (Saggese et al. 2020). Yungster et al. (2005) carried out both numerical and experimental studies in pulse detonation engines using hydrocarbon fuels. It was shown that NO_x formation in Jet A-fueled PDE can be controlled either using fuel-lean or rich mixtures and using the shortest possible detonation tube length. Schwer et al. (2016) also performed numerical simulations to evaluate NO_x emissions from air-breathing rotating detonation engines (RDEs). The paper provided much-needed insight into the NO_x emission from RDEs. Yungster et al. (2006) have conducted a numerical study on NO_x formation from a hydrogen-fueled PDE. They recommended using fuel-lean or fuel-rich mixtures to reduce NO_x emissions. They also mentioned the insensitivity

of NO_x emissions to residence time for very lean or very rich mixtures.

In the present analysis, the NO_x emission from Jet A fuel is investigated for varying flow conditions such as equivalence ratio, initial pressure, and initial temperature. In addition, NO_x emissions from stoichiometric Jet A–air detonations in the presence of inert diluents such as argon and helium are reported in the present work. Apart from NO_x concentrations, the detonation length and time scales, along with post-detonation temperature, are also reported in the present work. One-dimensional ZND computations were carried out using a detailed HyChem-NO_x model for Jet A, where predictions of NO_x concentrations were made using a detailed NO_x model from Glarborg et al. (2018).

Computational Methodology

One-dimensional ZND computations were carried out using CANTERA 2.4.0 integrated with MATLAB and Python (Goodwin et al. 2018). The Caltech Shock and Detonation Toolbox (Kao and Shepherd 2008; Browne et al. 2008) was used to compute the relevant ZND parameters. To model the combustion chemistry of Jet A, the HyChem model (Hybrid Chemistry) was used which is a physics-based model that contains the primary reaction pathways of liquid fuel. HyChem model combines a fuel pyrolysis model with a detailed foundational fuel chemistry sub-model to define the oxidation of decomposed products. With the NO_x chemistry included, the HyChem model consists of a total of 201 species and 1589 reactions. The Glarborg NO_x sub-model (Glarborg et al. 2018) was used to model the NO_x chemistry and was combined with the HyChem model to simulate Jet A–air detonations.

In a ZND model, the CJ detonation velocity is first computed using the input conditions such as P_0, T_0, and φ. Using the detonation velocity, normal shock relations are then used to compute the post-shock conditions such as pressure P_{VN}, temperature T_{VN}, density ρ_{VN}, and velocity u_{VN} in a shock-attached frame of reference. The structural evolution of the post-shock homogeneous mixture undergoing chemical reactions can then be traced by solving the conservation equations. The one-dimensional conservation equations that were solved numerically have been discussed in the literature elsewhere (Kumar and Singh 2021a, 2021b; Dahake et al. 2022a, b, c; Iyer et al. 2022b; Kumar et al. 2022a, b) and are given as follows:

Continuity:

$$\frac{d}{dx}(\rho u) = 0 \tag{1}$$

Species conservation:

$$\frac{d}{dx}\left(\rho u Y_k\right) = \omega_k W_k, k = 1, 2, \ldots .K \tag{2}$$

Momentum conservation:

$$\frac{d}{dx}\left(p + \rho u^2\right) = 0 \tag{3}$$

Energy conservation:

$$\frac{d}{dx}\left(h + \frac{u^2}{2}\right) = \frac{dh}{dx} + u\frac{du}{dx} = \sum_k (h_k \frac{dY_k}{dx} + Y_k c_{p,k}\frac{dT}{dx}) + u\frac{du}{dx} = 0 \tag{4}$$

$$h = \sum_k Y_k h_k(T) \tag{5}$$

Equation (5) represents the enthalpy per unit mass of the mixture.

$$h_k(T) = h^0_{f,k} + \int_{298K}^{T} c_{p,k} dT \tag{6}$$

The perfect gas approximation can be expressed as

$$p = \sum_k \rho Y_k R_k T = \rho\left(\sum_k Y_k R_k\right)T, R_k = \frac{R_u}{W_k} \tag{7}$$

Here, x represents the dimensional coordinate with the origin at the shock, Y_k is the mass fraction of species k, with $\sum_k Y_k = 1$. In Eqs. (1–7), K represents the total number of species, ω is the molar production rate, and W represents the molecular weight. The universal gas constant is $R_u = 8.314$ $\mathrm{Jmol^{-1}\,K^{-1}}$ and $W_k, R_k, c_{p,k}$, and $h^0_{f,k}$ represent the molecular weight, specific gas constant, specific heat, and the enthalpy of formation of the kth species, respectively. In addition, p, T, ρ, u, and h represent pressure, temperature, density, x-velocities, and enthalpy per unit mass of the mixture, respectively.

Once the structure of a detonation wave is established, the relevant length and time scales are calculated. The induction length (Δ_i) is defined as the distance between the leading shock front and the peak thermicity location. The location of peak thermicity also coincides with the location of the maximum temperature gradient [max(dT/dx)]. The time scale corresponding to the maximum rate of temperature rise [max(dT/dt)] or peak thermicity defines the induction time (τ_i). Thermicity is the transfer of energy from the reacting mixture's chemical bonds to the flow and thermal energy and gives the amount of energy released in the flow at a particular location behind the shock front (Kumar and Singh 2023; Ivin and Singh 2023). The post-shock temperature increases monotonically with the distance behind the shock. The maximum rate of temperature rise coincides with peak thermicity. The temperature then attains an equilibrium value after the reaction zone,

known as the CJ temperature or the post-detonation temperature. The post-detonation temperature (T_{CJ}) is the temperature of detonation products at the CJ plane. The post-detonation temperature governs the NO_x formation in a detonation wave. It is also an important parameter governing the operating limits of a detonation-based engine. The NO_x concentration reported in the present study is the sum of the concentration of individual oxides of nitrogen (NO, NO_2, N_2O) at the CJ plane.

The reaction zone length and time scales are the characteristic lengths and time scales for heat release based on chemical kinetics. The reaction zone includes the induction zone and extends to the final phase of heat release. Since the reaction zone length (Δ_r) gradually varies as a function of temperature, it is difficult to define the reaction zone length based on particular post-shock temperature rise, heat release rate, or the local Mach number in the shock frame of reference. Ng et al. (2005) defined reaction zone length as the ratio of the particle velocity of a steady CJ detonation in the shock-attached frame of reference to the maximum thermicity. Shepherd defined it based on the value of the local Mach number of 0.75 with respect to the wave frame of reference (Shepherd 1986). Similarly, Stamps et al. (1991) approximated the reaction zone length by the location where the Mach number reaches 0.9. However, a thorough analysis of reaction zone length using different definitions was carried out in the present work, and it was found that considering the fraction of heat release and temperature rise, reaction zone length can be approximated by the location where the Mach number reaches 0.9 since the total heat release, and the temperature rise is completed by the point where the Mach number reaches 0.9. Thus, the reaction zone length (Δ_r) in the present work is approximated by the location where the Mach number reaches 0.9, and the corresponding time scale is defined as the reaction time (τ_r). The recombination zone is the post-induction zone where three-body reactions are important and where the majority of heat release takes place. Thus, the reaction zone includes both the induction zone and the recombination zone. The different lengths and time scales used in the current work are defined as follows (Dahake and Singh 2021, 2022a, c, d; Singh et al. 2022):

$$\Delta_i = x|_{\dot{\sigma}_{\max}} \tag{8}$$

$$\tau_i = t|_{\dot{\sigma}_{\max}} \tag{9}$$

$$\Delta_r = x|_{M=0.9} \tag{10}$$

$$\tau_r = t|_{M=0.9} \tag{11}$$

$$\Delta_{recom} = \Delta_r - \Delta_i \tag{12}$$

$$\tau_{recom} = \tau_r - \tau_i \tag{13}$$

where x and t are the post-shock distance and time, respectively. Under detonating conditions, oxides of nitrogen are formed in the recombination zone. Thus, large recombination times can favor the higher production of nitrogen oxides as the species remains at high temperatures and pressure for a longer duration and vice versa. Particularly, large residence times, associated with large recombination times, increase the concentration of NO_x species. Thus, the recombination time (τ_{recom}) is indicative of the residence time and can be used to predict the NO_x emissions from a detonation wave.

Results and Discussions

Species Profiles of Nitrogen Oxides

One-dimensional ZND calculations were computed for stoichiometric Jet A–air detonation at 1 atm and 298 K. The species, temperature, and thermicity profile for a stoichiometric Jet A–air detonation are shown in Fig. 1. Behind the leading shock wave, Jet A first decomposes into a set of pyrolysis products due to high post-shock temperature. The adiabatic compression by the leading shock front heats the parent fuel molecule to autoignition temperature, where it readily decomposes into a set of pyrolysis products first. The key pyrolysis products of Jet A are C_2H_4, H_2, C_3H_6, i-C_4H_8, CH_4, C_2H_6, 1-C_4H_8, C_7H_8, and C_6H_6. The post-shock temperature is high enough (~ 1500 K) to facilitate such a decomposition. The oxidation of pyrolysis products occurs next and is the rate-limiting step. Figure 1 also shows that ethylene is the dominant pyrolysis species.

Towards the end of the oxidation zone, the intermediate pyrolysis species undergo oxidation with molecular oxygen leading to the production of H_2O, CO, and CO_2 and heat release. For the combustion of real fuel like Jet A, the pyrolysis zone and oxidation zone together represent the induction zone. Oxides of nitrogen such as NO, NO_2, and N_2O are produced in the recombination zone, where three-body reactions are prevalent and where a significant amount of heat release takes place. The recombination zone occurs after the induction zone. Reaction zone length in a ZND structure, therefore, includes both the induction and the recombination zone length. This length includes more than the induction zone and extends into the final phase of the heat release zone, where three-body reactions are prevalent. The induction zone length and ignition delay time for stoichiometric Jet A–air detonation was found to be 2.14 mm and 6.54 µs, respectively. It is to be noted that the pyrolysis process is fast when compared to the oxidation of decomposed products. This also enables to demarcate between the two zones in both the spatial and temporal scales. Thus, the rate-limiting step in the entire process leading to ignition is the oxidation process.

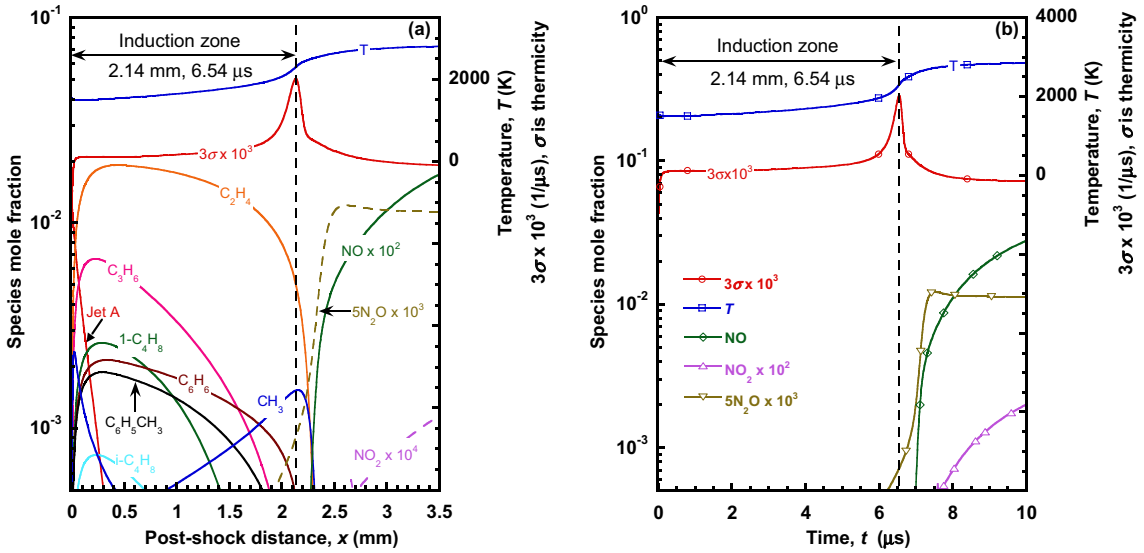

Fig. 1 **a** Major species profiles for stoichiometric Jet A–air detonation. **b** Species time history of nitrogen oxides (NO, N_2O, NO_2) for Jet A–air detonation. The calculations were carried out at $P_0 = 1$ atm, $T_0 = 298$ K, and $\varphi = 1.0$ using the combined HyChem-NO_x model for Jet A

It is observed that the concentration of NO (~ 500 PPM) is approximately two orders of magnitude larger as compared to the concentrations of NO_2 (~ 0.36 PPM) and N_2O (~ PPM). From Fig. 1b, it is observed that N_2O forms earlier than NO towards the end of the induction zone just after ignition. Downstream of the reaction zone, NO subsequently gets oxidized to NO_2 in the atmosphere. As the temperature at the end of the reaction zone (at the CJ plane) is very high, the formation of NO is favored by the thermal NO and the prompt NO mechanisms. Moreover, at high temperatures (> 800 K), the NO_2 formed is not stable. The main reaction pathway of NO_2 is through the reaction (14), where NO gets converted to NO_2:

$$NO + HO_2 \rightarrow NO_2 + OH \tag{14}$$

$$O + N_2(+M) \rightarrow N_2O\,(+M) \tag{15}$$

For the above reaction (14), the favorable temperature range of the reaction is less than 1000 K. At high temperatures, the NO_2 molecule is not stable, and it decomposes to NO. As for the formation of nitrous oxide (N_2O) is concerned, it is formed by the recombination of N_2 with atomic oxygen in the presence of a third body, as seen in reaction (15). However, N_2O may react with H or O to form NO or N_2 (see reactions 16–19). Here the NO-forming reactions compete with steps recycling N_2O to N_2:

$$N_2O + H \rightarrow NO + NH \tag{16}$$

$$N_2O + O \rightarrow NO + NO \tag{17}$$

$$N_2O + H \rightarrow N_2 + OH \tag{18}$$

$$N_2O + O \rightarrow N_2 + O_2 \tag{19}$$

The NH radical may further react with OH or O_2 to form NO or react with NO to form N_2 or N_2O. These competing steps may either lead to the production of NO or N_2O.

Effect of Varying Equivalence Ratio

The calculations were performed for the Jet A–air mixture at an initial temperature and initial pressure of 298 K and 1 atm, respectively. The NO_x concentrations (NO_x here includes NO, NO_2, and N_2O) were calculated for the case of equivalence ratio varying from 0.4 to 1.5. From Fig. 2a, the variation of detonation length and time scales with equivalence ratio can be seen. Both the induction zone length and time are found to be least at $\varphi = 1.1$. Correspondingly, post-detonation temperature T_{CJ} is maximum at $\varphi = 1.1$. In detonation studies, these length and time scales are important parameters as they can be empirically correlated to the cell size or width. Smaller length and time scales represent a strong coupling between the leading shock front and the reaction zone and quantitatively represent mixtures that are more detonable. The reaction zone length and time scales follow a similar trend with an equivalence ratio as the induction length and time scales.

In Fig. 2b, the variation of NO_x and the CJ detonation temperature with equivalence ratio is presented. It can be observed that near stoichiometric conditions, the NO_x concentration is maximum. At $\varphi = 1.0$, the NO_x concentration is

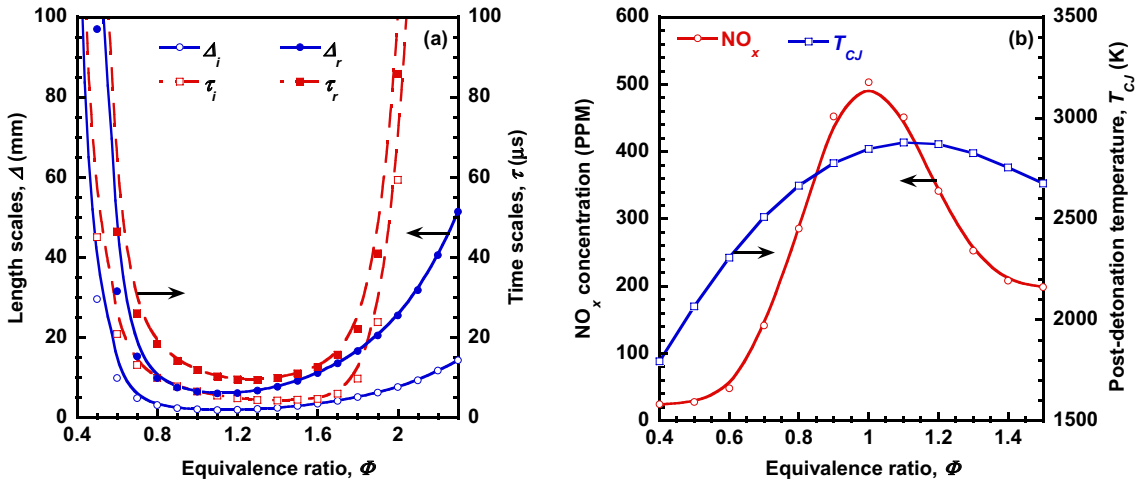

Fig. 2 Effect of variation of equivalence ratio (φ) on **a** the length and time scales and **b** the NO_x concentration and the post-detonation temperature (T_{CJ}) for Jet A–air detonations. The calculations were carried out at $P_0 = 1$ atm and $T_0 = 298$ K

close to 500 PPM. In addition, at stoichiometric conditions, the induction length is close to a minimum. For Jet A–air detonations at varying equivalence ratios, it is observed that NO_x concentration increases with increasing post-detonation temperatures, reaches a maximum around stoichiometric conditions, and then falls on the rich side.

This behavior is typical to that of post-detonation temperature, T_{CJ}. This is because thermal NO_x is a strong function of flame temperature in the reaction zone. Table 1 lists the values of post-detonation temperature, $T_{CJ,}$ where it can be seen that it first increases, reaches a maximum around $\varphi = 1.1$, and then decreases on the fuel-rich side. This influences the formation of $NO_{x,}$ where a similar trend can be observed in Fig. 2b. However, for both the fuel-lean and fuel-rich conditions, the concentration of NO_x is found to be relatively small when compared to stoichiometric conditions. For the fuel-lean mixtures, low values of post-detonation temperature (T_{CJ}) lead to low concentrations of NO_x. This is primarily because the dominant path to NO production in high-temperature gas combustion is thermal NO_x.

The effect of varying equivalence ratios on the NO_x emissions is shown in Fig. 2b. Although NO, NO_2, and N_2O contribute to NO_x concentration at a given equivalence ratio, it can be observed that NO is the most dominant species among the oxides of nitrogen for all equivalence ratios ranging from 0.4 to 1.5. It must be noted that the NO_x concentration can be reduced by an order of magnitude using fuel-lean mixtures. At the stoichiometric condition, the NO_x

Table 1 Detonation parameters and molar NO_x concentration for Jet A–air detonations with varying equivalence ratios at $P_0 = 1$ atm and $T_0 = 298$ K

φ	P_{VN} (atm)	T_{VN} (K)	M_{CJ}	P_{CJ} (atm)	T_{CJ} (K)	τ_i (μs)	τ_r (μs)	τ_{recom} (μs)	X_{NO} (PPM)	X_{N_2O}(PPM)	X_{NO_x}(PPM)
0.4	19.4	1120.2	4.1	10.5	1794.6	487.7	538.8	51.1	18.7	5.6	24.5
0.5	22.9	1238.2	4.4	12.2	2066.6	97.0	119.3	22.3	23.1	4.7	27.9
0.6	26.1	1337.9	4.7	13.9	2308.5	31.6	46.5	14.9	45.0	3.4	48.5
0.7	28.8	1418.1	4.9	15.4	2510.4	15.4	26.1	10.8	138.4	2.9	141.6
0.8	31.1	1478.7	5.1	16.7	2666.0	9.9	18.4	8.5	282.8	2.7	285.9
0.9	33.0	1522.4	5.3	17.8	2776.7	7.6	14.2	6.6	449.8	2.4	452.6
1	34.4	1551.9	5.4	18.6	2847.4	6.5	11.9	5.4	501.0	2.0	503.4
1.1	35.5	1568.3	5.5	19.1	2879.6	6.1	10.4	4.3	449.8	1.4	451.5
1.2	36.2	1571.3	5.5	19.3	2871.5	6.2	9.6	3.4	340.9	0.9	341.9
1.3	36.5	1561.7	5.5	19.2	2826.1	6.8	9.4	2.6	252.4	0.5	252.9
1.4	36.4	1543.2	5.5	19.0	2756.3	7.8	10.0	2.1	208.0	0.2	208.3
1.5	36.2	1520.0	5.5	18.7	2675.9	9.3	11.1	1.9	197.0	0.1	199.1

Only NO and N_2O concentrations are shown as they are the dominant species. NO_x concentration includes the total concentration of the oxides of nitrogen

concentration is ~ 503 PPM, which is more than twenty times the NO_x concentration at the fuel-lean condition ($\varphi = 0.4$). The NO_x concentration reduces as we move away from the stoichiometric condition, as shown in Fig. 2b. The reduction in NO_x concentration for fuel-lean conditions is due to decreasing post-detonation temperature (T_{CJ}) with equivalence ratio (refer to Fig. 2b and Table 1). However, the temperatures are comparable to the stoichiometric condition for the fuel-rich mixtures, but a substantial reduction in the NO_x concentration can be observed. The reason can be attributed to a competition between the excess fuel and nitrogen for the available oxygen. Thus, the available oxygen is preferentially consumed by the fuel resulting in oxygen deficiency for nitrogen oxidation to form nitrogen oxides. For all the cases considered, the amount of N_2O produced is much smaller than NO. It is observed that N_2O concentration increases at leaner equivalence ratios (see Table 1). The high concentration of N_2O is due to the presence of excess oxygen, where the recombination of nitrogen with atomic oxygen results in the formation of N_2O through the reaction (15). Similar results were also reported by Correa and Smooke (1991) for lean premixed laminar methane flames. This can be attributed to the N_2O-intermediate mechanism (see reaction (15)), which is important in fuel-lean conditions (typically for $\varphi < 0.8$).

The in situ method of operating a combustor at fuel-lean conditions to reduce NO_x emissions can be applied to detonation-based combustors and has been proposed by many researchers (Yungster and Breisacher 2005; Schwer and Kailasanath 2016; Yungster et al. 2006). However, operating detonation-based combustors under fuel-lean conditions can increase the detonation length and time scales drastically, as seen in Fig. 2a. The increase in the length and time scales indicates a loose coupling between the leading shock wave and the reaction zone. This can lead to the failure or attenuation of a detonation wave. In addition, the detonability of a given mixture is severely affected under fuel-lean conditions. Thus, NO_x reduction at fuel-lean conditions comes at the cost of a less detonable mixture that could affect the detonation wave structure and could lead to its attenuation or failure. These issues must be addressed before implementing the standard methods of NO_x reduction in detonation-based combustors.

Effect of Initial Temperature on NO_x Emissions

The NO_x emissions from stoichiometric Jet A–air detonations were computed for varying initial temperatures ranging from 300 to 1200 K at a constant pressure of 1 atm. Figure 3a, b represents the variation of length and time scales and NO_x concentrations with initial temperature. It is observed that induction length and time scales decrease with an increase in initial temperature (see Fig. 3a). This indicates an increased likelihood of detonation at higher initial temperatures. The post-shock temperature (T_{VN}) increases substantially with an increase in initial temperature at constant initial pressure (refer to Table 2). Since chemical kinetics is a strong function of post-shock temperature, an increase in post-shock temperatures results in faster decomposition of the parent fuel molecule. The oxidation of decomposed products also occurs faster due to increased reaction rates. The faster pyrolysis accompanied by rapid chemical reactions causes an overall decrease in the detonation length (Δ_i and Δr) and time (τ_i and τ_r) scales.

Figure 3b shows the variation of NO_x emissions with increasing initial temperature. It is observed that NO_x

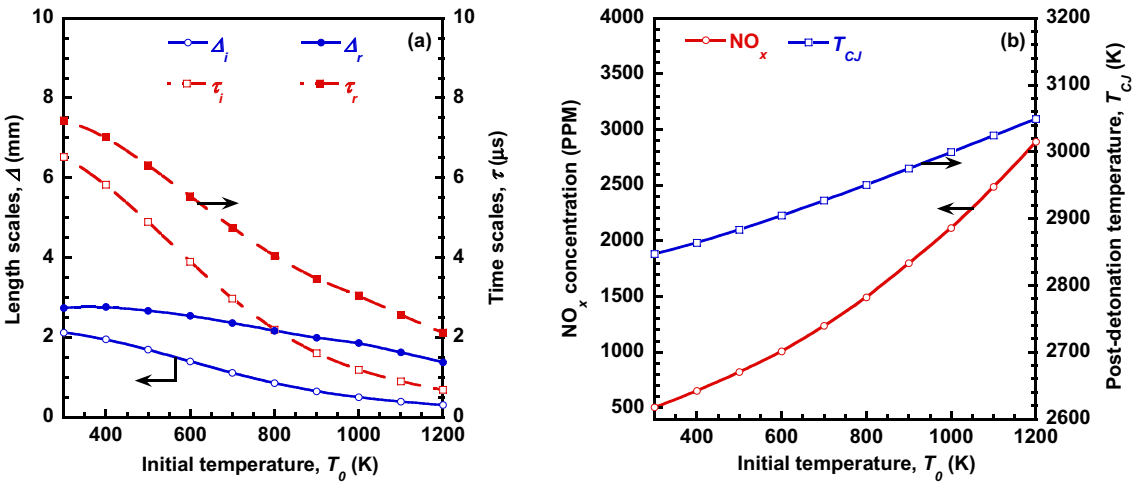

Fig. 3 Effect of variation of initial temperature (T_0) on **a** the length and time scales and **b** NO_x concentration and the post-detonation temperature (T_{CJ}) for stoichiometric Jet A–air detonation. The calculations were carried out at $\varphi = 1$ and $P_0 = 1$ atm

Table 2 Critical detonation parameters and molar NO_x concentration for Jet A–air detonation with varying initial temperature at $\varphi = 1$ and $P_0 = 1$ atm

T_0 (K)	P_{VN} (atm)	T_{VN} (K)	M_{CJ}	P_{CJ} (atm)	T_{CJ} (K)	τ_i (μs)	τ_r (μs)	τ_{recom} (μs)	X_{NO} (PPM)	X_{N_2O}(PPM)	X_{NO_x}(PPM)
300	34.4	1551.9	5.4	18.6	2847.4	6.5	7.4	0.9	501.0	2.0	503.4
400	25.7	1615.2	4.7	13.9	2863.8	5.8	7.0	1.2	652.1	1.8	654.4
500	20.4	1681.8	4.2	11.2	2883.2	4.9	6.3	1.4	820.5	1.7	822.7
600	16.9	1751.5	3.8	9.4	2904.5	3.9	5.5	1.6	1005.4	1.6	1007.6
700	14.4	1823.9	3.6	8.0	2927.1	3.0	4.7	1.8	1235.6	1.6	1237.8
800	12.6	1898.9	3.3	7.1	2950.7	2.2	4.0	1.8	1491.9	1.6	1494.2
900	11.1	1976.2	3.1	6.3	2974.9	1.6	3.5	1.9	1798.1	1.5	1800.5
1000	10.0	2055.6	3.0	5.7	2999.6	1.2	3.0	1.9	2113.0	1.5	2115.4
1100	9.0	2136.5	2.9	5.2	3024.5	0.9	2.6	1.7	2483.2	1.5	2485.8
1200	8.2	2218.4	2.7	4.8	3049.4	0.7	2.1	1.4	2888.9	1.5	2891.5

Only NO and N_2O concentrations are shown as they are the dominant species. NO_x concentration includes the total concentration of the oxides of nitrogen

concentrations are strongly dependent on the initial temperature. There is a drastic increase in NO_x concentration (~5.7 times) as the initial temperature is increased from 300 to 1200 K. As the initial temperature rises, both the post-shock temperature (T_{VN}) and the post-detonation temperature (T_{CJ}) increase significantly. Since thermal NO_x is the dominant mechanism for NO_x production, the concentration of NO increases significantly with an increase in post-detonation temperature leading to an overall increase in the production of NO_x. In addition, since the post-detonation temperatures are above 1000 K, the formation of NO_2 is very minimal. At such high temperatures, nitrogen dioxide (NO_2) will be readily decomposed to NO. Therefore, as the initial temperature increases, the NO concentration increases significantly.

The substantial increase in NO_x concentration is primarily due to an increase in the post-shock (T_{VN}) and post-detonation (T_{CJ}) temperatures. In addition, the recombination zone time increases with increasing initial temperature. Since the recombination zone time (τ_{recom}) is indicative of gas residence time, NO_x formation increases with increasing residence times. The increase in post-detonation temperature and residence time results in increased NO_x emissions. Therefore, NO_x concentration increases with increasing initial temperature due to higher post-detonation temperatures and residence times. For the temperature range tested above, it can be seen that the detonability of the Jet A–air mixture is increased along with an increase in NO_x emissions. Thus, at higher initial temperatures, although it is easier to sustain Jet A–air detonations, it comes at the cost of increased NO_x emissions.

Effect of Initial Pressure on NO_x Emissions

NO_x emissions for the case of varying initial pressure from 1 to 15 atm were carried out for stoichiometric Jet A–air detonations at an initial temperature of 298 K. The variation in induction zone length and time scales is also reported. Figure 4a, b presents the variation in detonation length and time scales and NO_x emissions with initial pressure. It is observed from Fig. 4a that an increase in initial pressure results in a decrease in the detonation length and time scales which quantitatively represent increased detonability. This is because of the pressure dependence of rate-limiting reactions. With the increase in initial pressure, the probability of binary collisions between molecules increases which in turn increases the reaction rates. The increased reaction rates cause both the length and time scales to vary inversely with the increasing pressure. It can be observed from Table 3 that increasing initial pressure leads to a very gradual increase in both the T_{CJ} and T_{VN}. Thus, an increase in post-shock temperature and CJ temperature with initial pressure also contributes to an increase in reaction rates which finally result in lower detonation length (Δ_i and Δ_r) and time (τ_i and τ_r) scales.

The NO_x emissions with varying initial pressure are shown in Fig. 3b. In the case of Jet A–air detonations, the NO_x emissions were found to decrease with the initial pressure. NO_x concentration decreases even though there is an increase in post-detonation temperatures, T_{CJ} with

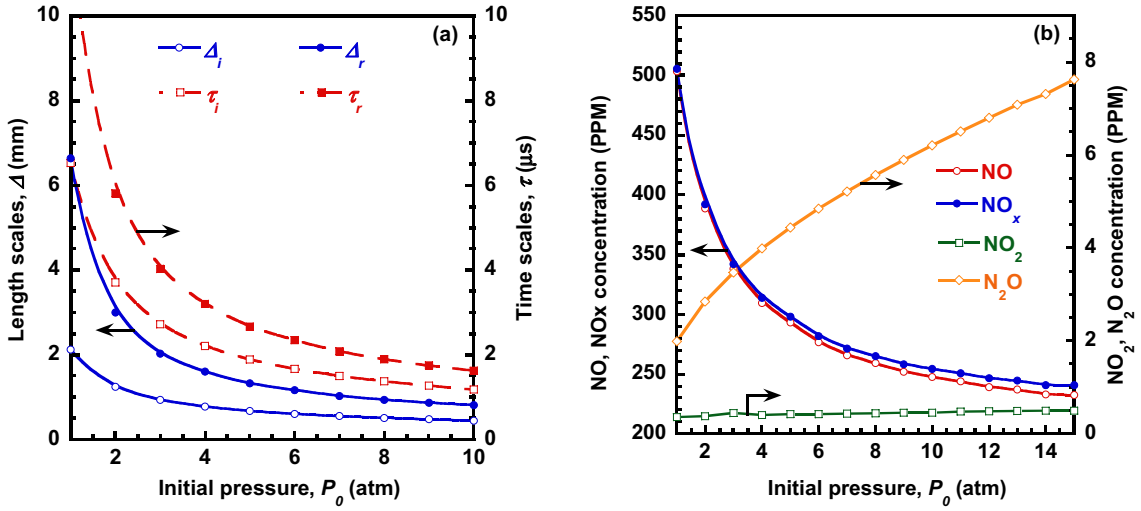

Fig. 4 Effect of variation of initial pressure (P_0) on **a** the length and time scales of a Jet A–air detonation and **b** NO_x concentration and its constituent species. The calculations were carried out at $\varphi = 1$ and $T_0 = 298$ K

Table 3 Detonation parameters and molar NO_x concentration for Jet A–air detonation with varying initial pressure (P_0) at $\varphi = 1$ and $T_0 = 298$ K

P_0 (atm)	P_{VN} (atm)	T_{VN} (K)	M_{CJ}	P_{CJ} (atm)	T_{CJ} (K)	τ_i (μs)	τ_r (μs)	τ_{recom} (μs)	X_{NO} (PPM)	X_{N_2O}(PPM)	X_{NO_x}(PPM)
1	34.7	1550.6	5.4	18.7	2847.4	6.5	11.9	5.4	501.0	2.0	503.4
2	70.3	1565.9	5.4	37.7	2890.4	3.7	5.8	2.1	388.8	2.8	392.0
3	106.2	1574.4	5.5	57.0	2914.6	2.7	4.0	1.3	338.2	3.5	342.1
4	142.4	1580.2	5.5	76.2	2931.2	2.2	3.2	1.0	309.4	4.0	313.8
5	178.6	1584.6	5.5	95.6	2943.8	1.9	2.7	0.8	293.0	4.4	297.9
6	215.0	1588.2	5.5	114.9	2953.8	1.7	2.3	0.7	276.5	4.8	281.7
7	251.5	1591.1	5.5	134.3	2962.2	1.5	2.1	0.6	265.7	5.2	271.4
8	288.1	1593.6	5.5	153.8	2969.4	1.4	1.9	0.5	259.0	5.6	265.0
9	324.7	1595.8	5.5	173.2	2975.5	1.3	1.7	0.5	251.8	5.9	258.2
10	361.4	1597.7	5.5	192.7	2980.5	1.2	1.6	0.4	247.5	6.2	254.2

Only NO and N_2O concentrations are shown as they are the dominant species. NO_x concentration includes the total concentration of the oxides of nitrogen

initial pressure. Although there is an increase in $T_{CJ,}$ which contributes to NO production via the thermal NO_x mechanism, in this case, the opposite trend can be observed. The numerical computations show that NO_x concentration decreases with an increase in initial pressure. It is observed that the NO_x concentrations are halved when the initial pressure is increased from 1 to 10 atm. The reason can be attributed to a corresponding decrease in the recombination zone time scale (τ_{recom}) (refer to Table 3 and Fig. 4a). As already discussed, the recombination zone time (τ_{recom}) is indicative of the gas residence time, which plays an important role in NO_x formation. It is seen that τ_{recom} decreases more than ~ 13 times when the pressure is increased from 1 to 10 atm. It is observed that NO_x concentration decreases with decreasing residence time. This is probably due to a decrease in the time available for the NO_x to form. Thus, there is a remarkable decrease in NO_x emissions as the residence time of gases decreases.

Asgari et al. (2018) have found similar results for syngas/air combustion where NO concentrations got reduced with increasing initial pressure. Hence, the drastic reduction in NO_x for the case of varying initial pressure may be attributed to a rapid drop in the recombination or residence time. This results in very little time available for the species to be in a state of higher temperature. Therefore, NO_x concentration decreases with increasing initial pressure due to shorter residence times.

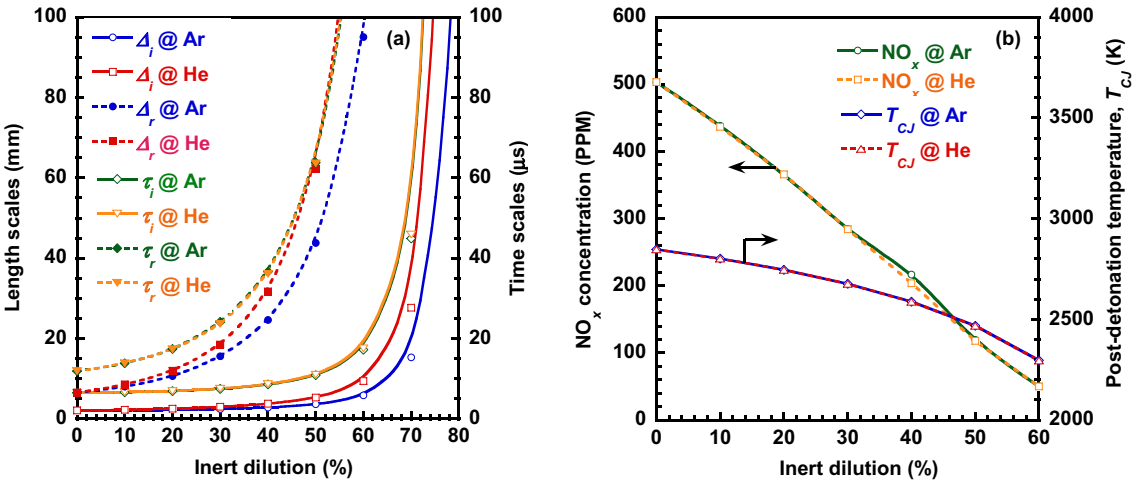

Fig. 5 Effect of variation of inert diluent concentration (molar %) on **a** the length and time scales for Jet A–air detonation and **b** NO_x concentration and the post-detonation temperature (T_{CJ}) for Jet A–air detonation. The calculations were carried out at $\varphi = 1$, $P_0 = 1$ atm, and $T_0 = 298$ K

Effect of Dilution on NO_x Emissions

ZND calculations were performed for Jet A–air detonations in the presence of inert diluents such as argon and helium. Inert diluents such as argon and helium are chemically inert and do not participate in chemical reactions. They have a strictly thermal-inhibiting effect on the detonation wave structure. The post-detonation temperature (T_{CJ}) decreases substantially with an increase in the molar concentration of the inert diluents (see Fig. 5b). The post-detonation temperature without diluents is high, ~ 2847 K, which is very high for practical applications of detonation-based combustors. However, it is observed that the addition of inert diluents such as argon and helium at 50% dilution decreases the post-detonation temperature to ~ 2588 K. This amounts to a ~ 9% decrease in the post-detonation temperature for both diluents. This is an important result as the post-detonation temperature governs the operating temperature limits of detonation-based combustors. This is a very favorable and promising result, but it severely affects the detonation length and time scales, and detonability limits of a given mixture (see Table 4). As seen from Fig. 5b, as we increase the concentration of inert diluents, the induction length increases significantly.

The addition of inert diluents affects the macroscopic detonation structure as it changes the relevant thermodynamic parameters for burned and unburned mixtures. Dilution reduces the exothermicity of the reacting mixtures, resulting in a smaller temperature rise in the reaction zone. The smaller temperature rise results in lower post-detonation temperatures. The reduction in exothermicity also reduces

Table 4 Critical detonation parameters and molar NO_x concentration for Jet A–air detonations with varying concentrations of inert diluents (molar-based %) at $P_0 = 1$ atm, $T_0 = 298$ K, and $\varphi = 1$

X_{Fuel}	X_{Ox}	X_{Ar} (%)	X_{He} (%)	P_{VN} (atm)	T_{VN} (K)	M_{CJ}	P_{CJ} (atm)	T_{CJ} (K)	τ_i (μs)	τ_r (μs)	τ_{recom} (μs)	X_{NO_x}(PPM)
0.0126	0.9874	0	0	34.4	1551.9	5.4	18.6	2847.4	6.5	11.9	5.4	503.4
0.0113	0.8887	10	0	33.5	1550.6	5.3	18.1	2847.1	6.7	13.9	7.2	438.2
0.0101	0.7899	20	0	32.3	1571.5	5.2	17.5	2801.2	7.0	17.4	10.5	365.3
0.0088	0.6912	30	0	30.8	1590.9	5.1	16.8	2745.8	7.5	24.2	16.6	284.5
0.0075	0.5925	40	0	29.2	1606.8	4.9	15.9	2676.9	8.6	36.7	28.1	216.9
0.0063	0.4937	50	0	27.2	1616.0	4.7	14.8	2588.1	10.9	63.8	52.9	119.6
0.0113	0.8887	0	10	33.5	1550.6	5.3	18.1	2847.1	6.7	13.9	7.2	436.8
0.0101	0.7899	0	20	32.3	1571.5	5.2	17.5	2801.2	7.0	17.4	10.4	365.9
0.0088	0.6912	0	30	30.8	1590.9	5.1	16.8	2745.8	7.6	23.7	16.2	284.3
0.0075	0.5925	0	40	29.2	1606.8	4.9	15.9	2676.9	8.7	36.1	27.5	203.7
0.0063	0.4937	0	50	27.2	1616.0	4.7	14.8	2588.1	11.1	63.7	52.6	117.9

NO_x concentration includes the total concentration of the oxides of nitrogen

the reaction rates and thus increases the reaction time. The increase in induction and reaction zone length is larger for helium than argon at the same dilution levels. Thus, argon is a better diluent than helium as the increase in induction and reaction zone length is small. It can be seen that the detonability drastically reduces for higher diluent percentages (> 50%). This is evident from the significant rise in both the length and time scales. Table 4 provides the data of detonation parameters and NO_x concentrations for stoichiometric Jet A–air detonations in the presence of argon and helium.

The effect of dilution on NO_x concentration can be observed in Fig. 5b. It is observed that the concentration of NO_x decreases continuously with increasing diluent concentration. It is worth mentioning that all oxides of nitrogen, namely NO, NO_2, and N_2O, decrease as the concentration of inert diluent increases (see Table 4). The reduction in NO_x concentration is similar for both the diluents, as the corresponding decrease in post-detonation temperature is nearly the same for argon and helium. Since argon and helium do not directly participate in chemical reactions, these do not directly influence NO_x concentration. The decrease is due to a corresponding decrease in the post-detonation temperature (T_{CJ}) with increasing dilution (refer to Table 4 and Fig. 5b). The insensitivity of NO_x towards the post-shock temperature (T_{VN}) can be seen in Table 4. The post-shock temperature (T_{VN}) increases up to 50% dilution and decreases thereafter. However, the NO_x emissions continue to decrease for all dilution levels. Thus, the NO_x formation is controlled by the post-detonation temperature (T_{CJ}) rather than the post-shock temperature (T_{VN}). This makes sense as the NO_x formation pathways occur primarily in the recombination zone, and as such, it is largely decoupled from the induction zone that precedes the recombination zone. Hence, the continuous reduction in NO_x across all dilution levels can be better explained by a decrease in T_{CJ}.

Conclusions

NO_x emissions from Jet A–air detonations were computed over a range of initial conditions. The HyChem model was combined with the Glarborg NO_x model and was used to model the combustion and NO_x chemistry of Jet A–air mixtures. The calculations were performed for varying flow conditions, such as with varying equivalence ratios, initial pressure, and initial temperature. It is observed that nitric oxide (NO) is the single most dominant species among the oxides of nitrogen, and its concentration is substantially higher than NO_2 and N_2O. The calculations show that NO_x emissions from a Jet A–air detonation can be reduced using fuel-lean mixtures. However, operating detonation-based combustors under fuel-lean conditions can increase the detonation length and time scales drastically. It is observed that nitric oxide is the dominant NO_x species and seems to govern the overall NO_x emission from Jet A–air detonations. The increase in initial pressure decreases the NO concentration while it increases the N_2O and NO_2 concentrations. NO_x concentration decreases with increasing initial pressure due to shorter recombination times and hence smaller gas residence times. NO_x concentration increases with increasing initial temperature due to higher post-detonation temperatures and residence times. The diluted Jet A–air mixtures produce less NO_x than the undiluted case primarily due to a reduction in the post-detonation temperature, T_{CJ}. The NO_x emissions from Jet A–air detonations show a strong dependence on the post-detonation temperatures and residence times.

Acknowledgements The financial support from Aeronautics Research and Development Board (ARDB) is gratefully acknowledged for the current work (Grant # ARDB/01/1042000M/I).

Data availability The authors confirm that the data supporting the findings of this study are available within the article. Raw data that support the findings of this study are available from the corresponding author, upon reasonable request.

References

Anand V, Gutmark E (2019) A review of pollutants emissions in various pressure gain combustors. Int J Spray Combust Dyn 02(01):1–18. https://doi.org/10.1177/1756827719870724

Asgari N, Padak B (2018) Effect of fuel composition on NOx formation in high-pressure syngas/air combustion. AIChE J. 64(08):3134–3140. https://doi.org/10.1002/aic.16170

Browne S, Ziegler J, Shepherd JE (2008) Numerical solution methods for shock and detonation jump conditions. Pasadena, CA

Correa SM, Smooke MD (1991) NOx in parametrically varied methane flames. Proc. Combust. Inst. 23(01):289–295. https://doi.org/10.1016/S0082-0784(06)80272-9

Chen GB, Li YH, Cheng TS, Hsu HW, Chao YC (2011) Effects of hydrogen peroxide on combustion enhancement of premixed methane/air flames. Int J Hydrog Energy 36(01):15414–15426. https://doi.org/10.1016/j.ijhydene.2011.07.074

Crane J, Shi X, Singh AV, Yujie T, Wang H (2018) Isolating the effect of induction length on detonation structure: Hydrogen–oxygen detonation promoted by ozone. Combust Flame 200(01):44–52. https://doi.org/10.1016/j.combustflame.2018.11.008

Dahake A, Singh AV (2021) Numerical study on NO_x emissions from a synthetic biofuel for applications in detonation-based combustors. AIAA Propul Energy Forum. https://doi.org/10.2514/6.2021-3678

Dahake A, Singh AV (2022a) A Comparative study of critical detonation parameters for jet a and an alcohol-to-jet synthetic biofuel. In AIAA Scitech. 18:022–0819

Dahake A, Singh AV (2022b) Effect of fuel sensitization on NO_x emissions from a synthetic biofuel under detonating conditions. In AIAA SCITECH. 51:022–0518

Dahake A, Singh AV (2022c) Nitrogen Oxides Emissions from Fuel-Sensitized Detonations for a Synthetic Biofuel. Trans Indian Natl Acad Eng. https://doi.org/10.1007/s41403-022-00354-y

Dahake A, Singh AV (2022d) A Comparative Study of the Detonation Chemistry and Critical Detonation Parameters for Jet A and a Biofuel. Trans Indian Natl Acad Eng. https://doi.org/10.1007/s41403-022-00353-z

Dahake A, Kumar DS, Singh AV (2022a) Using Ozone and Hydrogen Peroxide for Improving the Velocity Deficits of Gaseous Detonations. Trans Indian Natl Acad Eng. https://doi.org/10.1007/s41403-022-00345-z

Dahake A, Singh RK, Singh AV (2022b) Nitrogen Oxides Emissions from a Bio-derived Jet Fuel under Detonating Conditions. Trans Indian Natl Acad Eng. https://doi.org/10.1007/s41403-022-00378-4

Dahake A, Singh RK, Singh AV (2022c) NOx mitigation and Ignition Promotion Effects of Hydrogen Peroxide Addition to H_2-air. Trans Indian Natl Acad Eng. https://doi.org/10.1007/s41403-022-00374-8

Djordjevic N, Hanraths N, Gray J, Berndt P, Moeck J (2018) Numerical Study on the Reduction of NOx Emissions From Pulse Detonation Combustion. J Eng Gas Turbines Power 140(04):041504. https://doi.org/10.1115/1.4038041

Glarborg P, Miller JA, Ruscic B, Klippenstein SJ (2018) Modeling Nitrogen Chemistry in Combustion. Prog Energy Combust Sci 67(01):31–68. https://doi.org/10.1016/j.pecs.2018.01.002

Goodwin DG, Moffat HK, Speth RL (2009) Cantera: An object-oriented software toolkit for chemical kinetics. Pasadena, CA, Caltech. https://doi.org/10.5281/zenodo.48735

Hanraths N, Tolkmitt F, Berndt P, Djordjevic N (2018) Numerical study on NOx reduction in pulse detonation combustion by using steam injection decoupled from detonation development. J. Eng. Gas Turbines Power 140(12):121008. https://doi.org/10.1115/1.4040867

Ivin K, and Singh AV (2023) JP-10 Propellant Powered Rotating Detonation Waves for Enhancing the Performance of Hypersonic and Supersonic Missiles. In: G Sivaramakrishna (eds) Proceedings of the National Aerospace Propulsion Conference, Lecture Notes in Mechanical Engineering. Springer. Singapore

Iyer MSK, Singh AV (2022) Ignition Kinetics of Real Distillate Fuels Under Detonating Conditions. In Forum. https://doi.org/10.2514/6.2022-0816

Iyer MSK, Dahake A, Singh AV (2022) Comparative Studies on Ignition Kinetics and Detonation Chemistry of Real Distillate Fuels. Trans Indian Natl Acad Eng. https://doi.org/10.1007/s41403-022-00331-5

Kailasnath K (2000) Review of propulsion applications of detonation waves. AIAA J 10(2514/2):1156

Kumar DS, Singh AV (2021) Inhibition of hydrogen-oxygen/air gaseous detonations using CF_3I, H_2O, and CO_2. Fire Saf J 124(01):1–13. https://doi.org/10.1016/j.firesaf.2021.103405

Kumar DS, Ivin K, Singh AV (2021) Sensitizing gaseous detonations for hydrogen/ethylene-air mixtures using ozone and H_2O_2 as dopants for application in rotating detonation engines. Proc Combust Inst 38(03):3825–3834. https://doi.org/10.1016/j.proci.2020.08.061

Kumar DS, Dahake A, Singh AV (2022a) Detonation Chemistry of Fuel-Sensitized JetA1-Air Detonations. Trans Indian Natl Acad Eng. https://doi.org/10.1007/s41403-022-00339-x

Kumar DS, Dahake A, Singh AV (2022b) Detonation Chemistry of Fuel-Sensitized JetA1-Air Detonations. Trans Indian Natl Acad Eng. https://doi.org/10.1007/s41403-022-00339-x

Kumar DS, and Singh AV (2023) Using Ozone and Hydrogen Peroxide for Manipulating the Velocity Deficits, Detonabilility, and Flammability Limits of Gaseous Detonations. In: G. Sivaramakrishna (eds) Proceedings of the National Aerospace Propulsion Conference, Lecture Notes in Mechanical Engineering, Springer, Singapore

Magzumov AE, Kirillov I, and Rusanov V (1998) Effect of small additives of ozone and hydrogen peroxide on the induction-zone length of hydrogen-air mixtures in a one-dimensional model of a detonation wave. Combust Explos Shock Waves 34: 338–341. https://doi.org/10.1007/BF02672728

Ng HD, Radulescu MI, Higgins AJ, Nikiforakis N, Lee JHS (2005) Numerical investigation of the instability forone-dimensional Chapman-Jouguet detonations with chain-branching kinetics. Combustion Theory and Modeling 9(03):385–401. https://doi.org/10.1080/13647830500307758

Saggese C, Wan K, Xu R, Tao Y, Bowman CT, Park JW, Lu T, Wang H (2020) A physics-based approach to modeling real-fuel combustion chemistry–V. NOx formation from a typical Jet A. Combust Flame 212(01):270–278. https://doi.org/10.1016/j.combustflame.2019.10.038

Schwer DA, Kailasnath K (2016) Characterizing NO_x Emissions for Air-Breathing Rotating Detonation Engines. AIAA Propulsion Energy Forum. https://doi.org/10.2514/6.2016-4779

Shepherd JE (1986) Chemical Kinetics of Hydrogen-air-diluent Detonations. Prog Astronaut Aeronaut 106(01):263–293. https://doi.org/10.2514/5.9781600865800.0263.0293

Singh RK, Dahake A, Singh AV (2022) Inhibition of H_2-air Detonations Using Halogenated Compounds. Trans Indian Natl Acad Eng. https://doi.org/10.1007/s41403-022-00376-6

Stamps DW, Tieszen SR (1991) The Influence of Initial Pressure and Temperature on Hydrogen-Air-Diluent Detonations. Combust Flame 83(01):353–364. https://doi.org/10.1016/0010-2180(91)90082-M

Wang K et al (2018) A physics-based approach to modeling real-fuel combustion chemistry - IV HyChem Modeling of Combustion Kinetics of a Bio-derived Jet Fuel and its Blends with a Conventional Jet A. Combust Flame 198(01):477–489

Wang H, Xu R, Wang K, Bowman CT, Hanson RK, Davidson DF, Brezinsky K, Egolfopoulos FN (2018) A physics-based approach to modeling real-fuel combustion chemistry - I Evidence from experiments and thermodynamics, chemical kinetics, and statistical considerations. Combust Flame 193(01):502–519

Wang F, Weng C, Wu Y, Bai Q, Zheng Q, Xu H (2020) Numerical research on kerosene/air rotating detonation engines under different injection total temperatures. Aerosp Sci Technol 103(01):105899

Warimani M, Azami MH, Khan SA, Ismail AF, Saharin S, Ariffin AK (2021) Internal flow dynamics and performance of pulse detonation engine with alternative fuels. Energy 237(01):121719

Westbrook CK, Urtiew PA (1982) Chemical kinetic prediction of critical parameters in gaseous detonations. Proc Combust Inst 19(01):615–623. https://doi.org/10.1016/S0082-0784(82)80236-1

Westbrook CK (1982) Chemical kinetics of hydrocarbon oxidation in gaseous detonations. Combust Flame 46(01):191–210. https://doi.org/10.1016/0010-2180(82)90015-3

Xisto C, Petit O, Grönstedt T, Lundbladh A (2019) Assessment of CO_2 and NOx emissions in intercooled pulsed detonation turbofan engines. J. Eng. Gas Turbines Power 141(01):011016. https://doi.org/10.1115/1.4040741

Yungster S, Breisacher K (2005) Study of NO_x formation in Hydrocarbon-fueled Pulse Detonation Engine. Joint Propulsion. https://doi.org/10.2514/6.2005-4210

Yungster S, Radhakrishnan K, Breisacher K (2006) Computational study of NO_x formation in hydrogen-fuelled pulse detonation engines. Combust Theory Model 10(06):981–1002. https://doi.org/10.1080/13647830600876629

Zeldovich YB (1940) On the theory of the propagation of detonation in gaseous systems. J Tech Phys 10(01):542–568

Zhao M, Zhang H (2020) Origin and chaotic propagation of multiple rotating detonation waves in hydrogen/air mixtures. Fuel 275(01):117986

Zhao H, Yang X, Ju Y (2016) Kinetic studies of ozone assisted low-temperature oxidation of dimethyl ether in a flow reactor using molecular-beam mass spectrometry. Combust Flame

173(01):187–194. https://doi.org/10.1016/j.combustflame.2016.08.008

Publisher's Note Springer Nature remains neutral with regard to jurisdictional claims in published maps and institutional affiliations.

Springer Nature or its licensor (e.g. a society or other partner) holds exclusive rights to this article under a publishing agreement with the author(s) or other rightsholder(s); author self-archiving of the accepted manuscript version of this article is solely governed by the terms of such publishing agreement and applicable law.